Pergamon

Scripta Materialia, Vol. 40, No. 12, pp. 1353–1358, 1999
Elsevier Science Ltd

1359-6462/99/$–see front matter

PII S1359-6462(99)00122-0

EFFECTS OF GRAIN BOUNDARY ON SLIP MORPHOLOGY AND DISLOCATION PATTERNS IN A FATIGUED COPPER BICRYSTAL

Z.F. Zhang, Z.G. Wang and Y.M. Hu
State Key Laboratory for Fatigue and Fracture of Materials, Institute of Metal Research, Chinese Academy of Sciences, Shenyang, 110015, People's Republic of China

(Received March 30, 1999)
(Accepted April 15, 1999)

Keywords: Copper bicrystal; Cyclic deformation; Slip morphology; Dislocation patterns.

Introduction

By TEM technique, the fatigued dislocation structure in copper single crystals have been extensively investigated (1,2). It was found that the bulk of plastic strain was localized in those ladder-like persistent slip bands (PSBs) and the stress activating PSBs, i.e. the plateau stress, nearly maintained a constant value about 28–30 MPa (3,4). Afterwards, the ladder-like PSBs were also observed in the interior of the fatigued polycrystals (5), so the two-phase model proposed by Winter (6) was accepted in polycrystals. However, all the grains oriented randomly and grain boundaries (GBs) often led to elastic and plastic strain incompatibility in polycrystals during cyclic deformation. It should be very necessary to reveal the GB effect in polycrystals for better understanding the fatigue damage mechanism. Whereas, the TEM technique required thin foil specimens and the bulk specimen has to be destroyed. Sometimes, it is very difficult to examine the interactions of PSBs with GBs because the area observed by TEM is very small.

Recently, the electron channeling contrast (ECC) technique in SEM has been widely applied to study the dislocation patterns in deformed metals, such as nickel (7), copper (8), aluminum (9) and stainless steel (10). In particular, the SEM-ECC technique has many attractive features, for example, studying the dislocation arrangements over a large area and at some special sites of the specimen, including the vicinity of GBs, deformation bands (8) and cracks. To clarify the GB effect, bicrystal should be regarded as a very ideal model material. In our previous work (11), the interactions of PSBs with large- and low-angle GBs in copper bicrystal and multicrystal have been investigated. Wherein, the GB was perpendicular to the stress axis and secondary slip was not activated during cyclic deformation of the copper bicrystal. Therefore, the interaction of PSB with GB was relatively simple. Whereas, for the copper bicrystals with a parallel GB, the plastic strain incompatibility was rather serious and secondary slip or multiple slip was often activated near the GB, leading to a GB affected zone (GBAZ) during cyclic deformation (12,13). In this paper, the effect of GB on slip morphology and dislocation pattern

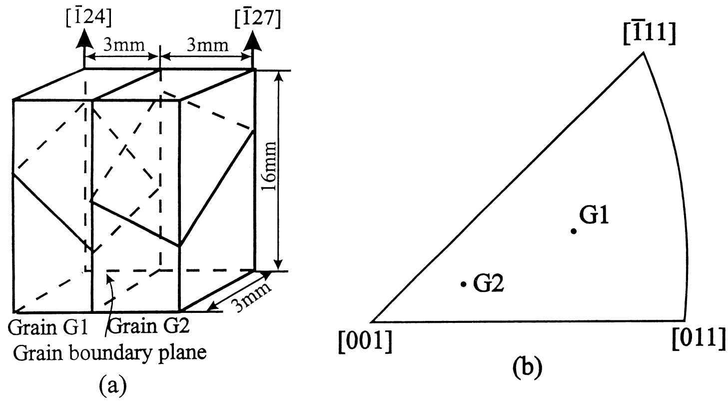

Figure 1. Fatigue specimen and component crystal orientations in a [$\bar{1}$24]/[$\bar{1}$27] copper bicrystal. (a) Fatigue specimen; (b) Crystal orientations in a stereographic triangle.

will be further investigated in a fatigued [$\bar{1}$24]/[$\bar{1}$27] copper bicrystal with the help of the SEM-ECC technique.

Experimental Procedure

A bicrystal with the size of $60 \times 20 \times 10$ mm^3 was grown from OFHC copper of 99.999% purity by the Bridgman method. A fatigue specimen with a parallel GB was made from the bicrystal plate, as shown in Fig. 1(a). By electron backscatter diffraction (EBSD) technique, the orientations of the two component crystals in the bicrystal were determined as follows

$$G1 = \begin{bmatrix} RD & TD & ND \\ 0.5929 & 0.2148 & 0.7761 \\ -0.2988 & -0.8362 & 0.4598 \\ 0.7478 & -0.5045 & -0.4316 \end{bmatrix} \quad \text{and} \quad G2 = \begin{bmatrix} RD & TD & ND \\ -0.7205 & -0.3056 & -0.6224 \\ -0.6134 & -0.1376 & 0.7777 \\ -0.3233 & 0.9422 & -0.0884 \end{bmatrix}$$

In brief, the bicrystal can be denoted as [$\bar{1}$24]/[$\bar{1}$27] and Fig. 1(b) gives the stress axis orientations of two crystals in the stereographic triangle. Clearly, both of two crystals are oriented for single slip. Before cyclic deformation, the bicrystal was electro-polished carefully for surface observation. Cyclic push-pull test was performed on a Shimadzu servo-hydraulic testing machine under constant plastic strain amplitude ($\Delta\epsilon_{pl}/2 = 5 \times 10^{-4}$) control at room temperature in air. A triangle wave with a frequency range of 0.1–0.5 Hz was used.

The peak loads in tension and compression were recorded continuously and the hysteresis loops were registered in intervals on an X-Y recorder until cyclic saturation occurred. After cyclic saturation, the slip morphology on the bicrystal surface was observed. Afterwards, those surface slip traces were removed and repolished to examine the dislocation patterns, especially near the GB, by the SEM-ECC technique.

Results and Discussion

During cyclic deformation, the bicrystal exhibited rapid cyclic hardening process, gradually reached cyclic saturation with an axial saturation stress of 67 MPa. Surface observations showed that only the

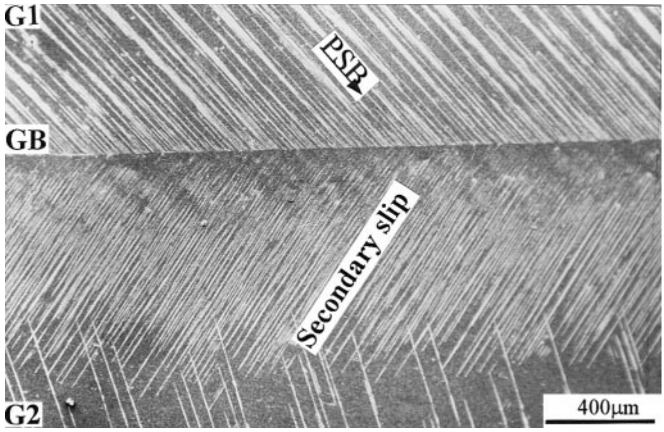

Figure 2. Surface slip morphology near the GB in the bicrystal cyclically deformed at strain amplitude of $\epsilon_{pl} = 5 \times 10^{-4}$ for 2×10^4 cycles.

primary slip bands were activated within the crystal G1. Similarly, on the component crystal G2 surface, there was also one group of slip bands apart from the GB. As shown in Fig. 2, it can be seen that those primary slip bands within crystal G2 could not reach the GB, but were terminated at certain distance from the GB. Meanwhile, instead of the primary slip bands, secondary slip bands appeared near the GB, forming a GB affected zone (GBAZ) with a width of 500–600 μm. It is indicated that there existed obvious plastic strain incompatibility near the GB in the bicrystal. In our previous work (12,13), a GBAZ containing secondary slip was also observed in [$\bar{1}$35]/[$\bar{1}$35], [$\bar{1}$35]/[$\bar{2}$35], [$\bar{2}$35]/[$\bar{2}$35] and [$\bar{6}$79]/[$\bar{1}$45] copper bicrystals. Whereas, the GBAZ in the [$\bar{1}$24]/[$\bar{1}$27] copper bicrystal is somewhat different from that in the above-bicrystals.

By the SEM-ECC technique, the ladder-like PSBs can also be observed in both crystals G1 and G2 after cyclic deformation of the bicrystal. In particular, those ladder-like PSBs within crystal G1 can extend to the GB continuously, and often became irregular near the GB. It is consistent with the surface slip morphology within crystal G1 in Fig. 2. However, the PSBs within crystal G2 gradually disappeared as they were close to the GBAZ. Instead of the ladder-like PSB structure, the dislocation pattern within the GBAZ became distinct labyrinth structure, as shown in Fig. 3. It is obvious that the

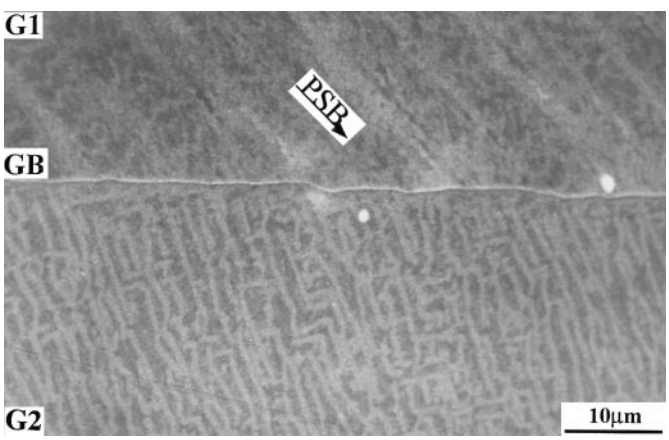

Figure 3. SEM-ECC micrograph of dislocation pattern near the GB.

dislocation pattern within the GBAZ is very different from that in [$\bar{1}$35]/[$\bar{1}$35] copper bicrystal (14,15), but is consistent with that in [001] copper single crystal (16,17). It means that ladder-like PSB structure can be changed into labyrinth structure owing to the operation of secondary slip in GBAZ. Whereas, the dislocation pattern within the GBAZ in [$\bar{1}$35]/[$\bar{1}$35] copper bicrystal was still the PSB structure, even though they became irregular near the GB. It may be reasonable that the [$\bar{1}$27] crystal is very close to the multislip oriented [001] crystal. However, the [$\bar{1}$35] and [$\bar{1}$24] crystals are typical single-slip orientations, as shown in Fig. 1(b). The operation of secondary slip system of the [$\bar{1}$27] crystal will be easier than that of [$\bar{1}$24] and [$\bar{1}$35] crystals owing to the GB effect during cyclic deformation. Therefore, the GBAZ containing secondary slip only appeared within the [$\bar{1}$27] crystal rather than the [$\bar{1}$24] crystal. In particular, it was concluded that labyrinth structure was a typical dislocation pattern in the [001] copper crystals during cyclic deformation (16,17). As a result, the dislocation pattern within the GBAZ in [$\bar{1}$27] crystal consisted of labyrinth structure rather than ladder-like PSB owing to the activation of secondary slip. Accordingly, the two-phase model proposed by Winter (6) might not be applied to the present bicrystal. It is indicated that the slip morphology and dislocation near a GB can also be affected by the orientation of the component crystal.

In addition to dislocation patterns and slip morphology, GB may also affect the saturation stress of the bicrystals. When a copper single crystal oriented for single-slip was cyclically deformed at the plastic strain range of plateau region, according Cheng and Laird model (4), its axial saturation stress σ_{as} will be equal to

$$\sigma_{as} = \tau_{as}^{PSB}/\Omega \tag{1}$$

where, τ_{as}^{PSB} is the stress activating PSBs and equal to 28–30 MPa (3,4), Ω is the Schmid factor of the primary slip system in the single crystal. If regardless of the GB effect, the axial saturation stress σ_{as}^{B} of the bicrystal should be equal to

$$\sigma_{as}^{B} = \sigma_{as}^{G1}V_{G1} + \sigma_{as}^{G2}V_{G2} = V_{G1}\tau_{as}^{PSB}/\Omega_{G1} + V_{G2}\tau_{as}^{PSB}/\Omega_{G2} = \tau_{as}^{PSB}(V_{G1}/\Omega_{G1} + V_{G2}/\Omega_{G2}) \tag{2}$$

Where, V_{G1} and V_{G2} are the volume fractions of the crystals G1 and G2 in the bicrystal, Ω_{G1} and Ω_{G2} are the Schmid factors of primary slip systems of the crystals $G1$ and $G2$ and equal to 0.486 and 0.490, respectively. Submitting $V_{G1} = V_{G2} = 0.5$, $\tau_{as}^{PSB} = 28–30$ MPa, $\Omega_{G1} = 0.486$ and $\Omega_{G2} = 0.490$ into eqn. (2), the axial saturation stress σ_{as}^{B} of the bicrystal should be in the range of 57.3–61.4 MPa. Obviously, the calculated saturation stress is smaller than that of the experimental value of 67 MPa, which can be attributed to the strengthening effect of GB or GBAZ.

Surface observations had revealed that the interaction of PSBs with the GB can lead to serious plastic incompatibility and the formation of labyrinth structure within the GBAZ during cyclic deformation. Recently, Gong et al (17) reported that the [001] copper crystals containing labyrinth structure always had a higher saturation stress than the single-slip-oriented crystal. In addition, Margolin *et al* (18), Rey and Zaoui (19,20) found that the increase in flow stress in β-brass and copper bicrystals can be attributed to GB strengthening effect during monotonic plastic deformation. For [$\bar{1}$35]/[$\bar{1}$35], [$\bar{1}$35]/[$\bar{2}$35], [$\bar{2}$35]/[$\bar{2}$35] and [$\bar{6}$79]/[$\bar{1}$45] copper bicrystals, their saturation stresses were also enhanced owing the presence of the GBAZ. Therefore, the GBAZ with labyrinth structure must play a strengthening role in the present copper bicrystal. Similarly, the saturation stress of the [$\bar{1}$24]/[$\bar{1}$27] copper bicrystal can be expressed as follows

$$\sigma_{as}^{B} = \sigma_{as}^{G1}V_{G1} + \sigma_{as}^{G2}V_{G2} + \sigma_{as}^{GB} \tag{3}$$

Where, σ_{as}^{GB} can be defined as the stress increase caused by the GBAZ and may be equal to 5.6–9.7 MPa. If introducing an orientation factor Ω_{B} of bicrystal (13)

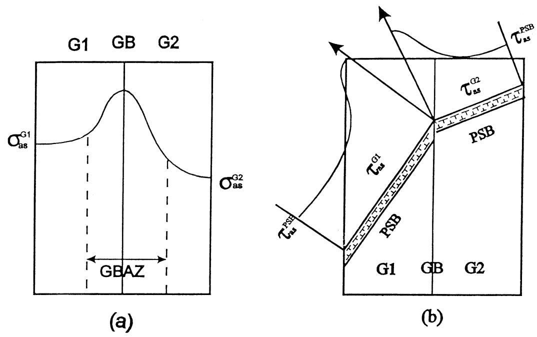

Figure 4. Diagrammatic sketch of GB strengthening effect in the bicrystal.

$$\Omega_B(V_{G1}/\Omega_{G1} + V_{G2}/\Omega_{G2})^{-1} \quad (4)$$

the saturation resolved shear stress of the bicrystal will be calculated as

$$\tau_{as}^{B} = \sigma_{as}^{B}\Omega_B = \sigma_{as}^{B}(V_{G1}/\Omega_{G1} + V_{G2}/\Omega_{G2})^{-1} = 32.7MPa \quad (5)$$

This stress is distinctly higher than 28–30 MPa of single-slip-oriented crystal. The increase in resolved shear stress of the bicrystal can be explained as the resistance of GB to PSBs during cyclic deformation. The diagrammatic sketch of GB strengthening effect in the bicrystal is illustrated in Fig. 4.

Conclusions

Serious plastic strain incompatibility near the GB was observed during cyclic deformation of a $[\bar{1}24]/[\bar{1}27]$ copper bicrystal. The slip morphology and dislocation pattern will be affected by the orientation of component crystal and the GB. As the orientation of the component crystal is close to [001] crystal, the dislocation pattern can be evolved into labyrinth structure owing to the GB effect, but not the ladder-like PSB structure. Whereas, in typical single-slip oriented component crystal, the ladder-like PSB structure still existed and only became irregular as they reached GB. Meanwhile, a relatively higher saturation stress (32.7 MPa) was observed compared with the single-slip oriented crystal, if modified by an orientation factor Ω_B of bicrystal. The increase in saturation stress of the bicrystal should be attributed to the GB strengthening effect or the resistance of GB to PSB. The results above might be very necessary to further understanding the fatigue behavior of polycrystals.

Acknowledgment

This work was financially supported by the National Natural Science Foundation of China (NSFC) under grant numbers 19392300-4 and 59701006. The authors are grateful for those supports.

References

1. C. Laird, P. Charsley, and H. Mughrabi, Mater. Sci. Eng. 81, 433 (1986).
2. Z. B. Basinski and S. J. Basinski, Prog. Mater. Sci. 36, 89 (1992).
3. H. Mughrabi, Mater. Sci. Eng. 33, 207 (1978).
4. A. S. Cheng and C. Laird, Mater. Sci. Eng. 51, 111 (1981).
5. A. T. Winter, Acta Metall. 28, 963 (1980).

6. A. T. Winter, Phil. Mag. A30, 719 (1974).
7. J. Bretschneider, C. Holste, and B. Tippelt, Acta Mater. 45, 3755 (1997).
8. B. Gong, Z. Wang, D. Chen, and Z. G. Wang, Scripta Mater. 37, 1605 (1997).
9. D. R. G. Mitchell and R. A. Day, Scripta Mater. 39, 923 (1998).
10. R. Zauter, F. Petry, M. Bayerlein, C. Sommer, H-J. Christ, and H. Mughrabi, Phil. Mag. 66, 425 (1992).
11. Z. F. Zhang and Z. G. Wang, Phil. Mag. Lett. A78, 105 (1998).
12. Y. M. Hu and Z. G. Wang, Mater. Sci. Eng. A208, 260 (1996).
13. Z. F. Zhang and Z. G. Wang, Acta Mater. 46, 5063 (1998).
14. Y. M. Hu and Z. G. Wang, Mater. Sci. Eng. A234–236, 98 (1997).
15. Y. M. Hu and Z. G. Wang, J. Mater. Sci. Lett. 17, 865 (1998).
16. N. Y. Jin and A. T. Winter, Acta Metall. 32, 1173 (1984).
17. B. Gong, Z. R. Wang, and Z. G. Wang, Acta Mater. 45, 1365 (1997).
18. Y-D. Chuang and H. Margolin, Metall. Trans. A4, 1905 (1973).
19. C. Rey and A. Zaoui, Acta Metall. 28, 93 (1980).
20. C. Rey and A. Zaoui, Acta Metall. 30, 523 (1982).